Cr(III) Complexes Bearing a -Ketoimine Ligand for Olefin Polymerization: Are There Differences between Coordinative and Covalent Bonding?

catalysts

MDPI

Article

Cr(III) Complexes Bearing a β-Ketoimine Ligand for Olefin Polymerization: Are There Differences between Coordinative and Covalent Bonding?

Alessia Amodio [1], Giorgia Zanchin [2,*], Fabio De Stefano [3], Alessandro Piovano [1], Benedetta Palucci [2], Virginia Guiotto [1], Rocco Di Girolamo [3], Giuseppe Leone [2] and Elena Groppo [1]

[1] Dipartimento di Chimica, NIS Interdepartmental Research Center and INSTM Reference Center, Università degli Studi di Torino, I-10135 Torino, Italy; alessia.amodio@unito.it (A.A.); alessandro.piovano@unito.it (A.P.); virginia.guiotto@edu.unito.it (V.G.); elena.groppo@unito.it (E.G.)
[2] Consiglio Nazionale delle Ricerche, Istituto di Scienze e Tecnologie Chimiche "Giulio Natta" (SCITEC), I-20133 Milano, Italy; benedetta.palucci@scitec.cnr.it (B.P.); giuseppe.leone@scitec.cnr.it (G.L.)
[3] Dipartimento di Scienze Chimiche, Università di Napoli "Federico II", Complesso Monte S. Angelo, I-80126 Napoli, Italy; fabio.destefano@unina.it (F.D.S.); rocco.digirolamo@unina.it (R.D.G.)
* Correspondence: giorgia.zanchin@scitec.cnr.it

Abstract: β-ketoimines are extensively applied for the synthesis of organometallic complexes intended as (pre)catalysts for a variety of chemical transformations. We were interested in the synthesis of two Cr complexes bearing a simple bidentate β-ketoimine (**L**), with different ligand binding modes, as well as their application as a precatalyst in the polymerization of olefins. Complex **1** (L_2CrCl_3) was obtained by direct reaction of **L** with $CrCl_3(THF)_3$, while, for the synthesis of complex **2** ($LCrCl_2$), the ligand was first deprotonated with *n*BuLi, giving the β-ketoiminato ligand $\mathbf{L^-Li^+}$, and then reacted with $CrCl_3(THF)_3$. Characterization of the complexes proved that the Cr(III) ion is coordinatively bonded to **L** in **1**, while it is covalently bonded to **L** in **2**. The complexes were then used as precatalysts for the polymerization of ethylene and various cyclic olefins. Upon activation with methylaluminoxane, both the complexes exhibited poor activity in the polymerization of ethylene, whilst they exhibit good productivity in the polymerization of cyclic olefins, affording semicrystalline oligomers, without a significant difference between **1** and **2**. To gain more insight, we investigated the reaction of the complexes with the Al-cocatalyst by IR and UV-Vis spectroscopies. The results proved that, in case of **1**, the Al-activator deprotonates the ligand, bringing to the formation of an active species analogous to that of **2**.

Keywords: chromium β-ketoimine complexes; catalysis; homogeneous catalysts; polyolefins; poly(cyclic olefins)

Citation: Amodio, A.; Zanchin, G.; De Stefano, F.; Piovano, A.; Palucci, B.; Guiotto, V.; Di Girolamo, R.; Leone, G.; Groppo, E. Cr(III) Complexes Bearing a β-Ketoimine Ligand for Olefin Polymerization: Are There Differences between Coordinative and Covalent Bonding? *Catalysts* **2022**, *12*, 119. https://doi.org/10.3390/catal12020119

Academic Editor: Zhiqiang Fan

Received: 24 December 2021
Accepted: 17 January 2022
Published: 19 January 2022

1. Introduction

Among the family of bidentate OˆN ligands, we can number the β–ketoimines, [1] which are structurally analogous to the ubiquitous β-diketones [2] and β-diketimines, [3] as schematically represented in Figure 1.

Recently, all these ligands have gained profound interest from a broad perspective of coordination chemistry by virtue of their tunable electronic and steric features. They have been extensively used in coordination chemistry as supporting ligands [3] and are especially prominent in catalysis for olefin polymerization, [4–7], small-molecule activation chemistry, [8–13] and as ancillary ligands for phosphorescent molecules [14–17].

The coordination ability of β-diketones (left in Figure 1), such as acetylacetone, is well established and a large number have been synthesized as ligands to form complexes with various metals. Metal β-diketonates have been known since the nineteenth century; [18] from that moment on, their synthesis, and physical and chemical properties have been

described in hundreds of papers and several reviews [19,20]. Many transition metal complexes have been obtained with the bidentate ligand acetylacetonate (acac), in which typically both oxygen atoms bind to the metal to form a six-membered chelate ring. The simplest complexes have the formula $M(acac)_3$ and $M(acac)_2$, where M can be both an early or a late transition metal [2,20]. However, tuning of the steric and electronic properties of this ligand can be accomplished only by modifications of the R substituents on the ligand backbone (Figure 1).

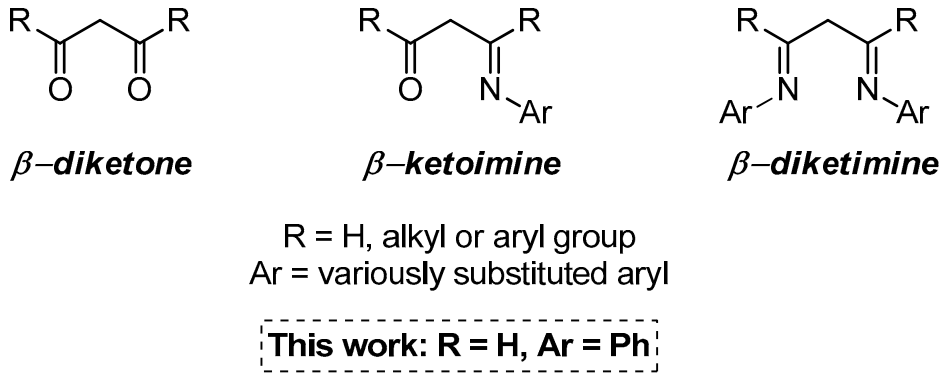

Figure 1. β-diketone, β-ketoimine and β-diketimine ligands.

On the opposite side, in the β-diketimine ligands (right in Figure 1) it is possible to tune not only the R substituents, but also the aryl (Ar) ring, as well as to variate the bonding modes, ranging from purely σ to a combination of σ and π donation depending on the steric environment and the electron demand at the bound metal [3,5,7,14,16,21,22]. These peculiarities make β-diketimines good candidates to stabilize various metal ions in multiple oxidation states and coordination numbers. However, the steric bulkiness of β-diketimines is a double-edged sword: indeed, despite being advantageous for the stability, it can be unfavorable because it may significantly hinder the metal center [23]. Therefore, it is desirable to introduce some unsymmetrical features into the ligand framework to have enough steric protection, but not that much that limits the substrate access to the catalytic pocket. In this context, the β-ketoimine ligands (middle in Figure 1), structurally related to the previously cited ligands but with properties in-between the two, may serve as a suitable ligand framework, able to target both the issues of enhancing the complex stability and reducing the steric bulkiness [1].

β-ketoimines are formed by the condensation of primary amines with β-diketones or β-ketoaldehydes. They have been less investigated with respect to their isoelectronic analogs β-diketones and β-diketimines [14–16,24–28]. Beyond being largely exploited for the preparation of organic light-emitting diodes (OLEDs), [29] there are some examples of metal complexes with β-enaminoketonato chelate ligands employed as single component initiators for the ring-opening polymerization of cyclic esters, [25] or as precatalysts for the polymerization of (cyclic) olefins [24].

In this context, as a part of an ongoing study on chromium catalysts for olefin polymerization, [30,31] we were interested in studying Cr(III) complexes bearing β-ketoimine ligands. Some papers appeared in the recent literature reporting on the synthesis of chromium complexes with similar ligands; [6,7,21,28] the interest in these bidentate chromium complexes have developed since they can be considered homogeneous models of the heterogeneous Phillips catalyst, and hence they help to improve the understanding of the underlying organometallic chemistry. However, to the best of our knowledge, Cr-complexes bearing β-ketoimine ligands have never been reported before, in contrast to the huge amount of literature present for other related chromium complexes, as comprehensively reviewed by Sun et al. [32].

Herein, we report on the synthesis, characterization, and catalytic testing of two Cr(III) complexes with a β-ketoimine ligand, obtained from two different synthetic routes:

coordination and covalent bonding of the ligand with the metal. The complexes were characterized by IR and UV-Vis spectroscopies, also in the presence of the Al-cocatalyst. Finally, upon activation with methylalumoxane (MAO), they were evaluated as catalysts for the polymerization of ethylene, and some cyclic olefins (namely, norbornene (NB), dicyclopentadiene (DCPD), 5-ethylidene-2-norbornene (ENB), 3,5-norbornadiene (NBD)). Combining all the provided data, we tried to set out if there are any differences among the complexes, as they are and as active catalysts for olefin polymerization.

2. Results and Discussion

2.1. Synthesis of the Complexes

The ketoimine ligand **L** was synthesized in good yield by condensing the 2,4-pentanedione with the aniline, according to a published procedure [33]. Successively, the ligand **L** was reacted employing two different procedures with a chromium(III) salt in dry THF at room temperature to give the desired complexes **1** and **2** (Scheme 1): for complex **1**, the ligand **L** was directly reacted with $CrCl_3(THF)_3$, giving a green powder in 78% yield, while in the case of complex **2**, the β-ketomine **L** was previously deprotonated with an equimolar amount of *n*BuLi, giving the β-ketoiminato ligand $\mathbf{L^-Li^+}$, and then reacted with $CrCl_3(THF)_3$ to afford a brownish solid in 92% yield. In the latter case, the Cr-cation is expected to be covalently bonded to the deprotonated ligand $\mathbf{L^-}$. The detailed synthesis procedure is reported in the experimental section. Both the complexes are soluble in THF, chloroform, and dichloromethane, fairly soluble in toluene, while insoluble in common alkanes. They are air and moisture sensitive, thus requiring characterization under strictly inert conditions.

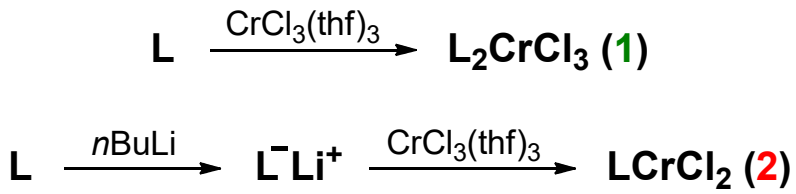

Scheme 1. Schematic representation of the two synthetic routes.

–Elemental analysis for complex **1** well matches with two ligand molecules for each Cr atom according to the stoichiometry L_2CrCl_3, while for complex **2** elemental analysis matches with the stoichiometry $LCrCl_2$, with only one ligand molecule and two Cl^- ions per Cr atom (Scheme 1). Unfortunately, despite repeated attempts, we were unable to obtain suitable single crystals, thus preventing their structural characterization by X-ray diffraction. For this reason, the complexes were thoroughly characterized by IR and UV-Vis spectroscopies, which together have the potential to provide information on the Cr coordination mode.

2.2. Characterization of the Bare Complexes

Figure 2 shows the IR spectra of the two complexes compared to that of the ligand, in the most significant spectral regions. The interpretation of the IR spectra is not straightforward, because of the extended resonance in the ring systems.

Before discussing the spectra of the complexes, it is important to assign the main absorption bands in the spectrum of the ligand. It is known that it can undergo keto-enolic and imine-enamine equilibria, resulting in a tautomeric mixture of structures I, II, and III shown in Figure 3.

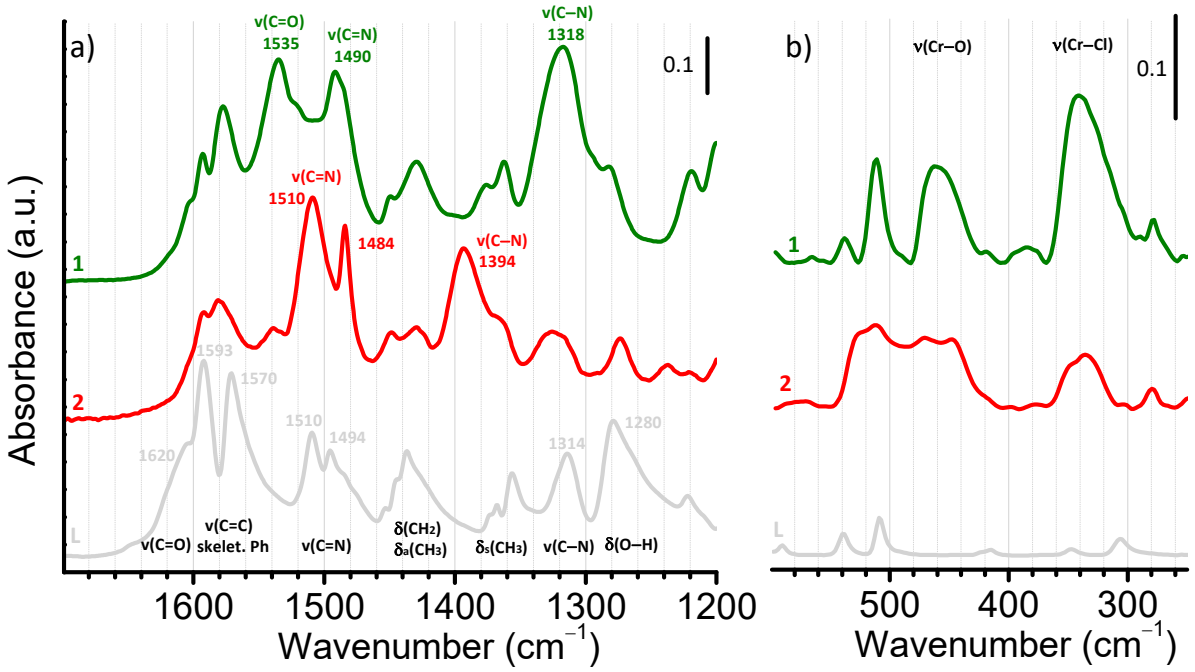

Figure 2. ATR-IR (**a**) and Far-IR (**b**) spectra of complexes **1** (green line) and **2** (red line) in comparison to that of the ligand **L** (grey line)in the most relevant spectroscopic regions. Measurements were performed on complexes in the solid state.

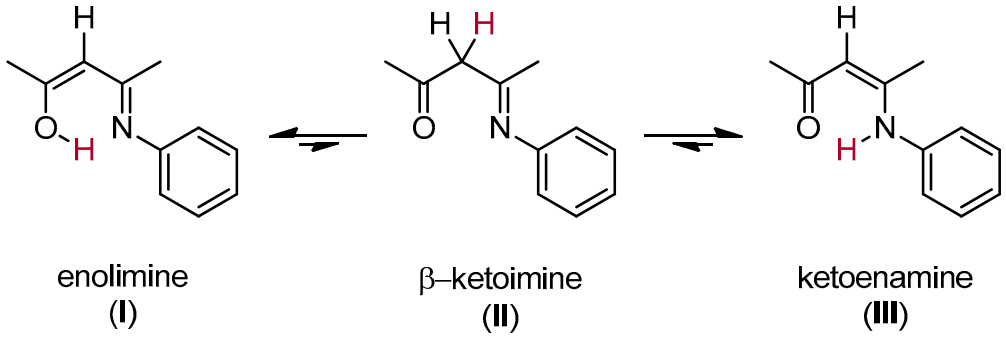

Figure 3. Tautomers of L ligand: structures I and III containing –OH and –NH groups are greatly stabilized by intra- and intermolecular hydrogen bonding and are expected to be predominant.

Theoretically, structures I and III are predominant since the hydrogen bonding that is formed either between the hydroxyl hydrogen and the imine nitrogen (I) or between the amine hydrogen and the carbonyl oxygen (III), as well as the greater resonance, stabilize these structures over structure II. However, a clear distinction between structure I and III has been difficult to accomplish, since the equilibrium among them can be influenced by several factors, such as the polarity of the solvent in which the sample is dissolved. The ^{1}H NMR spectrum recorded in deuterated tetrachloroethane shows a preference for the enolimine form (structure I) (Figure S1). At the same time, the IR spectrum of the solid sample (Figure 2) is the superposition of the spectra corresponding to the two structures, with strong absorptions in the regions corresponding to ν(C=C) and ν(C=N) for structure I, and ν(C=C) and ν(C=O) for structure III, demonstrating that structures I and III are both possible. It is important to notice that, since the double bonds are conjugated and the hydrogen-bonded structures are characterized by a certain degree of resonance, these double bonds have considerable single bond character and contribute at frequencies lower than usual [34]. The absence of bands in the 1700–1620 cm^{-1} region confirms that structure II (with non-interacting C=O and C=N groups) is not present.

In more detail, the first absorption band (shoulder) in the 1620–1600 cm^{-1} region is assigned to ν(C=O) vibration for the hydrogen-bonded carbonyl of structure III. The next absorption in the 1600–1560 cm^{-1} region is assigned to ν(C=C) stretching vibrations in both structures I and III. The two bands at 1593 and 1570 cm^{-1}, separated by a dip at 1580 cm^{-1}, most likely originate from a Fermi resonance with an intense band due to skeletal vibrations of the phenyl ring. The set of bands around 1500 cm^{-1} is ascribed to ν(C=N) vibration for the hydrogen-bonded imine of structure I, overlapped with another skeletal vibration of the phenyl ring at 1494 cm^{-1}. The set of bands below 1460 cm^{-1} are common to both structures I and III: the bands in the 1460–1340 cm^{-1} region are due to the deformation modes of CH_2 and CH_3 groups, the one at 1314 cm^{-1} is assigned to ν(C–N) of the N–Ph group, while that at 1280 cm^{-1} is ascribed to the O–H deformation vibration in the hydrogen-bonded rings [34]. Finally, in the Far-IR region (Figure 2b) the ligand contributes only with very weak bands.

The IR spectra of the two complexes greatly differ from that of the ligand and are also different from each other, suggesting that Cr coordination occurs in two different fashions, depending on whether the Cr salt is chelated by the neutral ligand **L** or by its deprotonated form $\mathbf{L}^-$. Typically, when the metal is coordinated by the neutral ligand, a prototropy from N/O to the γ-C occurs (Scheme 2, left) [35]. This explains the main changes observed in the spectrum of complex **1** with respect to that of the ligand **L**. In particular, the spectrum is now dominated by three very intense bands, at 1535, 1490, and 1318 cm^{-1} (Figure 2a). The former is attributed to ν(C=O) vibration for the metal chelated carbonyl, in good agreement with the relatively low C=O bond order found in metal chelates of metallic acetylacetonates [34] and metallic bisacetylacetone-ethylenebisimine complexes [36]. The band at 1490 cm^{-1} is attributed to ν(C=N) stretching: it is almost unperturbed in terms of frequency with respect to the same band in the spectrum of **L** but is strongly enhanced in intensity, as already reported for metallic bisacetylacetone-ethylenebisimine chelate complexes [36]. Finally, the strong and broad band at 1318 cm^{-1} is tentatively ascribed to the ν(C–N) vibration of the N–Ph group, which is enhanced in intensity due to a much larger polarization of the bond induced by the presence of the metal. In the Far-IR region (Figure 2b), the spectrum is dominated by two intense and broad bands at 460 and 340 cm^{-1}, which are straightforwardly attributed to ν(Cr–O) and ν(Cr–Cl) vibrations [37]. There is no evidence of bridged chlorine species (the corresponding ν(Cr–Cl) vibration is expected around 280 cm^{-1}). The two narrow bands at 538 and 512 cm^{-1} are assigned to the vibrational modes of the ligand in the complex, enhanced in intensity with respect to those of the neutral ligand **L**.

In contrast, the deprotonated $\mathbf{L}^-$ is a bidentate monoanionic OˆN ligand analog and isoelectronic with the β-diketonato (such as acac) and β-diketiminato (such as nacnac) ligands. Metallation of $\mathbf{L}^-$ should occur according to one of the structures schematically shown in Scheme 2 (right). The IR spectrum of complex **2** (Figure 2a) indicates that structure (**M-I**) is the most probable one. In fact, the spectrum is characterized by two very intense bands at 1510 cm^{-1} (ν(C=N) vibration) and 1394 cm^{-1} (ν(C–N) vibration of the N–Ph group), both enhanced in intensity by the presence of the covalently bonded Cr cation, while no bands are observed in the spectral region characteristic for the ν(C=O) vibration of the metal chelated carbonyl. In the Far-IR region (Figure 2b), the spectrum is similar to that of complex **1**, albeit the ν(Cr–Cl) band is weaker and the ν(Cr–O) band is broader.

All in all, the detailed analysis of the ATR-IR spectra of the two complexes, coupled with the information derived from elemental analysis, allowed us to advance a hypothesis on their structure as schematically shown in Figure 4. It is worth noticing that complex **2** is similar to the dichloride complex $(Ph)_2(nacnac)CrCl_2(thf)_2$ reported by Theopold and co-workers, synthesized following a very similar procedure [6]. According to ATR-IR spectroscopy, THF residuals are not present in both complexes.

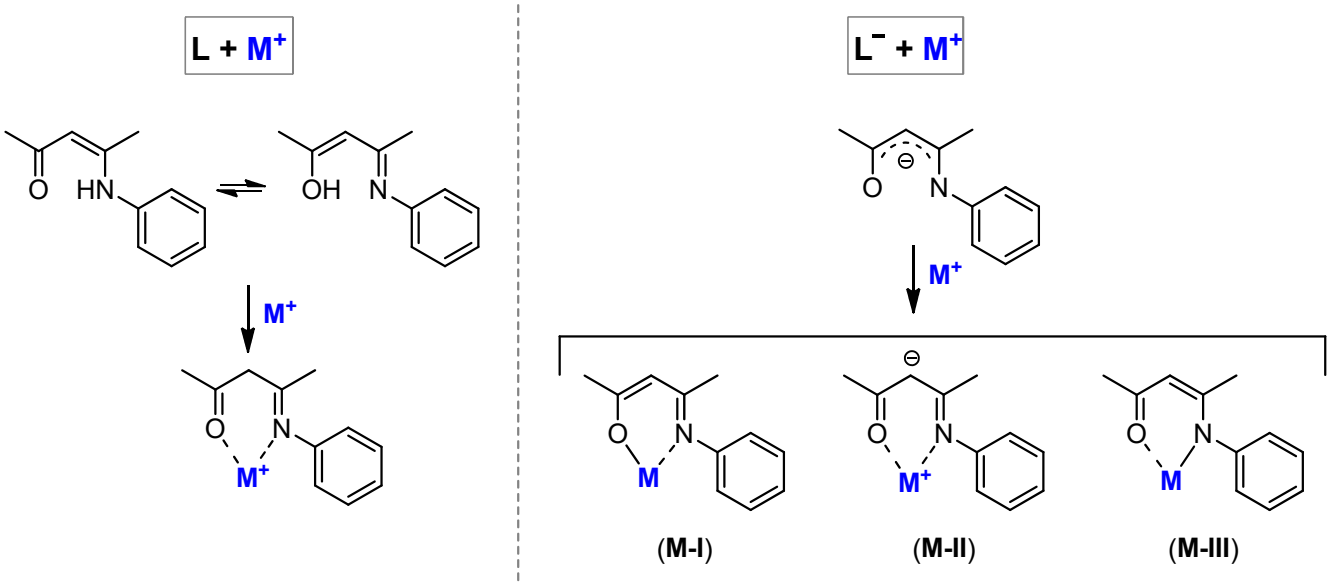

Scheme 2. Schematic representation of the ligand, both in the neutral (**L**, left) and in the deprotonated ($\mathbf{L}^-$, right) form, chelating a metal M^+. For simplicity, additional ligands and/or halogens in the metal coordination sphere are omitted.

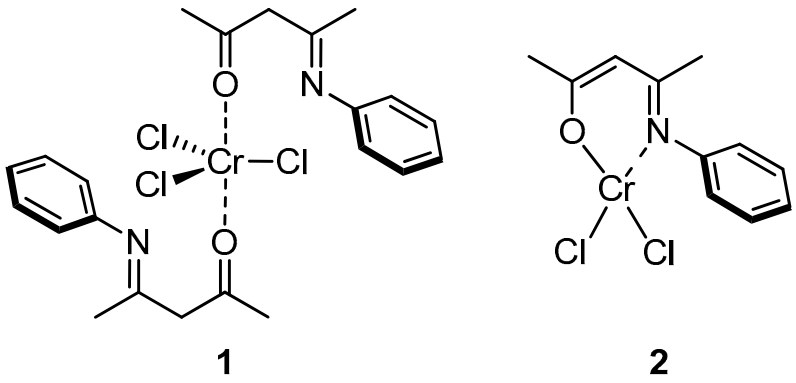

Figure 4. Schematic representation of the molecular structure of the two Cr-based ketoiminato complexes, as determined by ATR-IR spectroscopy coupled with elemental analysis. The C=N and C=O bonds have been localized according to the IR results. Full lines indicate covalent bonds, while dashed and dotted bonds indicate ionic interactions of decreasing strength.

The UV-Vis spectroscopy data are in agreement with the structures reported in Figure 4. Figure 5 compares the UV-Vis spectra of the two complexes with that of the ligand, both in the region characteristic for the intra-ligand π-π* transitions (part a) and in that characteristic for Cr d-d transitions. The spectra have been collected at two different concentrations in the two regions of interest to optimize the signals without saturating the detector.

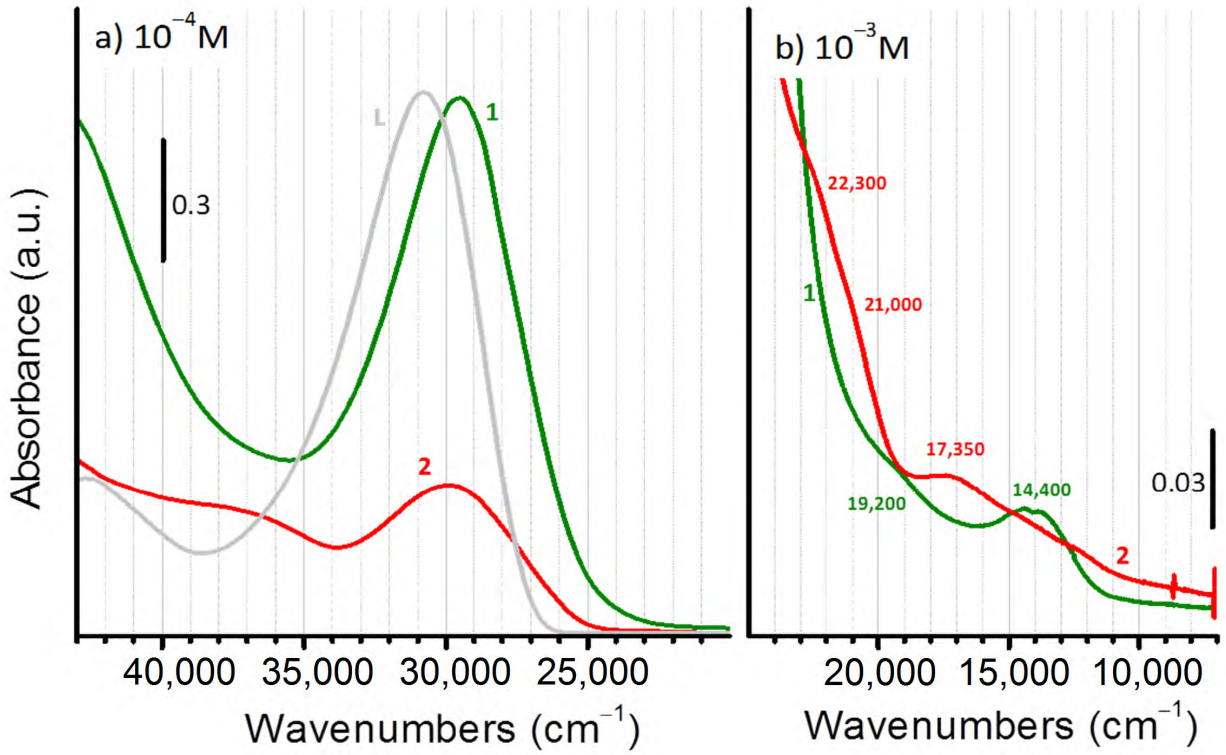

Figure 5. Transmission UV-Vis spectra of complexes **1** (green line) and **2** (red line) in comparison to that of the neutral ligand **L** (grey line) in the region of intra-ligand π-π* transitions (**a**) and in the region of d-d transitions (**b**). The spectra have been collected in chloroform at the concentration of 10^{-4} M (**a**) and 10^{-3} M (**b**), respectively.

In the spectrum of the neutral ligand **L**, the π-π* transition at the lowest energy is observed at about 30,800 cm^{-1}. Metallation of the ligands causes a bathochromic shift of this band, slightly larger for complex **1** (29,600 cm^{-1}) than for complex **2** (30,000 cm^{-1}). In addition, the spectrum of complex **2** shows a broad band centered at about 37,000 cm^{-1}, which is tentatively assigned to an O → Cr ligand-to-metal charge-transfer transition, which can be observed only when Cr is covalently bonded to O. In the region characteristic for d-d transitions, two bands are observed for complex **1** around 14,400 and 19,200 cm^{-1} as typically observed for highly coordinated Cr(III) complexes, such as those having an octahedral coordination or slightly lower symmetry (including penta-coordinated ones) [38]. The energy position of these bands is sensitive to the ligands, according to the spectrochemical series. For example, values as low as 18,700 and 13,200 cm^{-1} have been found for $CrCl_6$, whereas the same bands are observed at 24,500 and 17,400 cm^{-1} for $Cr(H_2O)_6$. Intermediate values are observed for complex **1**, as expected for the presence of both Cl and O ligands in the Cr coordination sphere.

The spectrum of complex **2** is more complicated, since both d-d bands are split into two components and shifted to higher energy (at about 22,300, 21,000, 17,350, and 12,600 cm^{-1}). According to the crystal field theory, a split in d-d transition is expected when the octahedral geometry is distorted. In particular, by moving toward a square planar coordination, a split of both bands into two components is predicted, [39] which is what is observed in the present case. As far as the shift in energy is concerned, this is explained by the spectrochemical series of the ligands, [38] considering that, with respect to complex **1**, in complex **2** a Cl atom is substituted by an O atom in the Cr coordination sphere.

2.3. Polymerization Tests

2.3.1. Ethylene

The catalytic utility of **1** and **2** was first investigated in the polymerization of ethylene. Both the complexes were used as precatalyst in combination with different aluminum alkyls (i.e., Et_2AlCl, Et_3Al, MAO, and $AlMe_3$-depleted MAO (dMAO)) as cocatalysts (Table S1). Both the chromium complexes were weakly active for ethylene polymerization. Only traces of solid polyethylene (PE) were recovered, also by varying the polymerization conditions, i.e., temperature, solvent, and amount of the Al-activator. Despite the low activities, the molecular weight of the PEs produced by precatalyst **1** in combination with Et_2AlCl and MAO are quite high, with relatively broad molecular weight distribution ($6.0 < M_w/M_n < 9.5$). The melting temperatures (T_ms) are in the range 132–137.5 °C, and the crystallinity of these polymers is in the range 60–70% (Table S1). The X-ray diffraction profiles of all the synthesized PE samples show two peaks at 2θ values of 21° and 24°, corresponding to the orthorhombic form of crystalline PE (Figure S2). All these data are in agreement with highly linear and high-molecular weight polymers.

2.3.2. Cyclic Olefins

We were later interested in testing **1** and **2** as precatalysts in the polymerization of NB and other derivatives, namely, DCPD, ENB, and NBD (Figure 6). Cyclic olefin polymers have high thermal resistance and chemical stability, becoming attractive candidates for a wide variety of applications such as gas-separation and proton-conducting membranes, microelectronics, photoresists, dielectric materials, and pervaporation applications [40,41]. Polymerization conditions and results are summarized in Table 1.

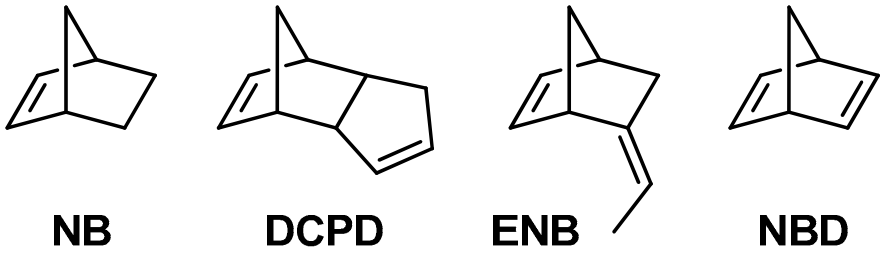

Figure 6. Cyclic olefins employed as monomers in this study.

Table 1. Polymerization of NB, DCPD, ENB, NBD promoted by **1–2** precatalysts.[a]

Entry	Monomer	Complex	T (°C)	Yield (g)	Yield (%)	M_w [b] (g mol^{-1})	M_n [b] (g mol^{-1})	M_w/M_n [b]
1	NB	1	20	1.05	78	1790	1055	1.7
2	NB	2	20	1.00	74	1740	1210	1.4
3	NB	1	0	1.20	89	1990	1080	1.8
4	NB	2	0	1.20	89	2330	1385	1.7
5	DCPD	1	20	0.32	13	1140	880	1.3
6	DCPD	2	20	0.30	13	1140	855	1.3
7	ENB	1	20	1.98	92	2320	1420	1.6
8 [c]	NBD	1	20	1.21	73		insoluble	

[a] Polymerization conditions: [monomer] = 1 mol L^{-1} (that is, NB, 1.35 g, DCPD, 2.36 g, ENB, 2.16 g, NBD, 1.66 g); total volume, 18 mL (toluene); t = 24 h; Cr, 10 μmol; MAO as cocatalyst, Al/Cr = 1000. [b] M_w, M_n, and M_w/M_n by SEC. [c] reaction stopped at 10 min.

When activated with MAO, both the complexes are active in the polymerization of NB, affording solid polymers (Table 1, entry 1 and 2). The conversion of NB was in the range 74−78% at room temperature, while reaching 89% for the same experiment at 0 °C (Table 1, entry 3 and 4). Surprisingly enough, the monomer conversion in the polymerizations performed with **1**/MAO and **2**/MAO are comparable. On the contrary, when Et_2AlCl was

employed as cocatalyst (not shown in Table 1), **1** and **2** gave no activity. An analogous result was recorded in the case of iminopyridine chromium complexes by some of the authors [30]. The molecular weights of the polymers obtained are all in the range from 1050 to 1400 g mol^{-1} (M_n in Table 1), meaning that the resultant materials are oligomers constituted by a few repeating units (7–15 units), with narrow molecular weight distribution ($1.4 < M_w/M_n < 1.8$).

When DCPD, the bicyclic analogue of NB, was polymerized, a steep reduction in the monomer conversion, as low as 13% for both complexes, was recorded (Table 1, entry 5 and 6). The large steric hindrance of DCPD may account for the low insertion-coordination rate of DCPD, and hence for the low productivities. The molecular weight is rather low: the DCPD oligomers are made up of a few (less than 10) repeating units. Similar results were obtained in the polymerization of DCPD catalyzed by Cr-iminopyridine complexes [42].

Conversely, the polymerization of ENB brings an increase of monomer conversion up to 92% (Table 1, entry 7), even higher than that of NB. In this case, the presence of the second double bond, i.e., the ethylidene moiety on the C5 of NB ring, may have a beneficial effect, probably binding the active species and making it more reactive and prone toward polymerization.

Finally, concerning the polymerization of the non-conjugated NBD, a different situation occurred: the reaction was extremely rapid and exothermic, and the viscosity of the reaction medium increased so rapidly that the polymerization was stopped within 10 min, with monomer diffusion issues limiting the conversion to 73% (Table 1, entry 8). Note that the resultant powder sample was insoluble, even at high temperatures, thus making impossible to determine its molecular weight.

2.3.3. Cyclic Olefin Oligomers Characterization

The cyclic olefin oligomers obtained were characterized with the aid of different techniques to get information on their structure, that is monomer enchainment, and therefore on the possible different polymerization mechanisms involved. In fact, cyclic olefins can be polymerized by three different catalytic routes (Scheme 3): (i) ring-opening metathesis polymerization (ROMP), which gives polymers containing double bonds within the main chain, (ii) vinyl addition polymerization, which gives completely saturated polymer, and (iii) cationic polymerization, which gives low-molecular weight products containing rearranged monomer units [40,43].

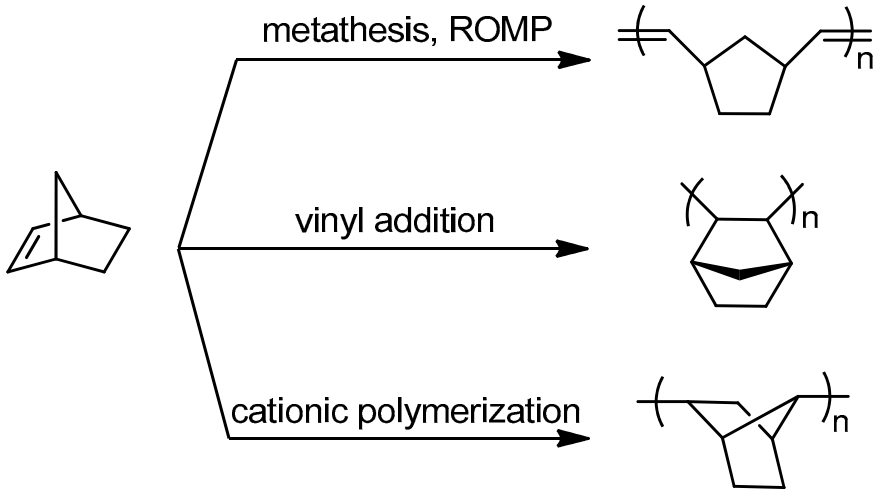

Scheme 3. Schematic representation of the types of NB polymerization.

The characterization of the polymers by IR and NMR spectroscopy showed that the polymerization of NB, DCPD, and ENB mediated by the catalytic system **1**–**2**/MAO occurs through a vinyl-type addition rather than via ROMP, in analogy with the results previously obtained by some of the authors with other Cr-catalysts [30,44].

The IR spectra of NB oligomers show characteristic absorption bands at 2942, 2865, 1451, 1294, 1110, and 891 cm^{-1} (Figure S3). The selective occurrence of addition polymerization via opening of only the endocyclic double bond is well demonstrated by the absence of any band at 1680−1620 cm^{-1}, characteristic of the unsaturated NB ring [44].

The IR spectra of both the DCPD and ENB oligomers (Figure S4) show the typical signals of the norbornenic ring, as observed in the spectrum of pure NB (2940, 2910, 2865, 1450, 1268, 1100 cm^{-1}), and in addition the signals of the double bonds, that is the =C–H stretching at 3040 cm^{-1} and the C=C stretching at 1650–1680 cm^{-1}. The presence of bands at 3040 (=C–H stretching vibration) and 1613 cm^{-1} (C=C stretching vibration) and the absence of any band at about 1580 cm^{-1} indicate that all the bicycloheptene double bonds were consumed during the oligomerization [45]. The remaining unsaturations are entirely due to the cyclopentene double bond or to the ethylidene moiety, which are not involved in the polymerization [30].

This was further confirmed by the ^{1}H and ^{13}C NMR spectra of the oligomers (Figures S5 and S6). The ^{13}C NMR spectra of both the oligomers present many and broad peaks in the region spanning from 30 to 50 ppm, that, by structural analogy with NB, can be assigned to the carbon atoms belonging to the norbornenic ring [42,46]. The presence of signals in the olefinic region (at 128–132 ppm for DCPD oligomers, and at 110 and 145 ppm for ENB oligomers) further demonstrates that the polymerization occurs through vinyl addition, and does not involve the pendant double bond.

The structure of all synthesized oligomers reported in Table 1 was characterized by wide angle X-ray scattering diffraction (WAXD). WAXD profiles of all the NB oligomers are shown in Figure 7: all the samples are semi-crystalline as indicated by the presence of two main broad reflections centered at 2θ values of 11.5 and 18.5°, according to the 2,3-*exo*-diheterotactic polyNB structure [30,44]. Moreover, samples corresponding to entry 1, 2, and 3 (profiles a, b, c of Figure 7) present an extra diffraction peak at 2θ = 11.2° probably related to structural disorder or polymorphism present in these samples.

Thermogravimetric analysis of NB oligomeric samples, performed under a N_2 atmosphere, is reported in Figure S7. TGA curves revealed that all these samples are stable up to ≈350 °C (T_{onset}) and then progressively start decomposing at higher temperatures.

The X-ray investigation of the obtained DCPD oligomer (Figure 8) demonstrates that the sample is crystalline. The diffraction profile is superimposable to that of the previously reported semicrystalline DCPD oligomers [42]. With regard to the chain stereochemistry of the DCPD oligomers obtained, it was possible to speculate that they have the same 2,3-*exo*-diheterotactic stereoregularity found in the case of the polyDCPD and polyNB obtained with a chromium iminopyridine catalyst [30].

A different situation was encountered when characterizing the polyNBD (Table 1, entry 8). Indeed, the analysis of the solid powder by means of IR and X-ray diffraction demonstrated the formation of an unusual structure with rigid nortricyclene repeating units and a unique 3,5-enchainment (Scheme 4).

The IR spectrum (Figure S8) clearly shows the presence of a sharp and very strong band at 802 cm^{-1}, attributable to the C–H stretching of a cyclopropylic ring (i.e., 2,6-disubstituted nortricyclene structure) [47], and the concomitant absence of a band at about 1580 cm^{-1}, characteristic of the double bond of the norbornenic ring. On the other side, the X-ray powder diffraction profile of the sample (Figure 9) proves that it is crystalline, as indicated by the presence of Bragg diffraction peaks at 2θ values of 13.7, 16, and 20.4°.

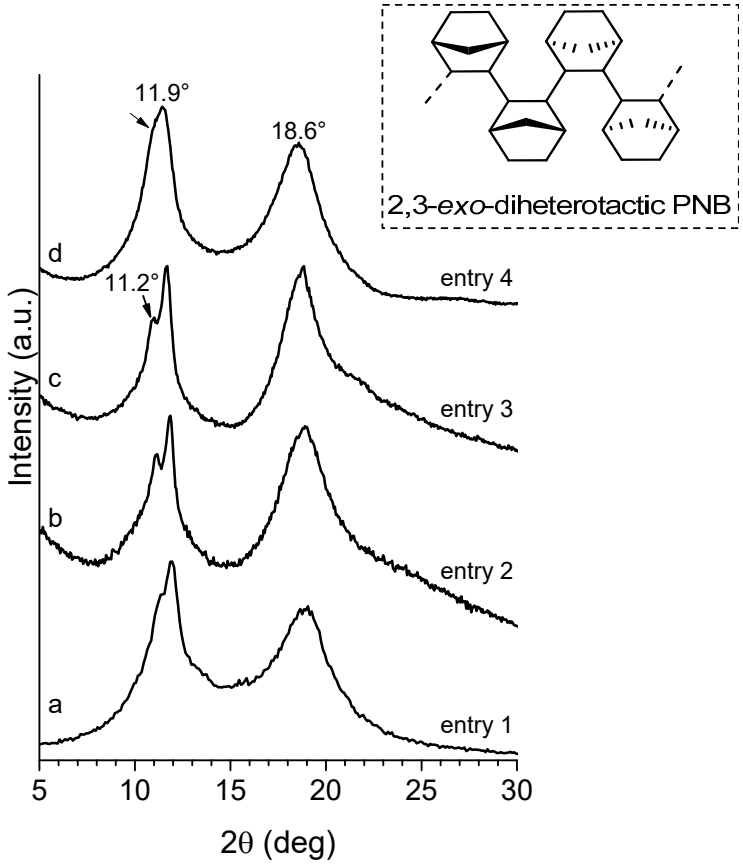

Figure 7. X-ray powder diffraction profiles of the as-prepared NB oligomer samples reported in Table 1.

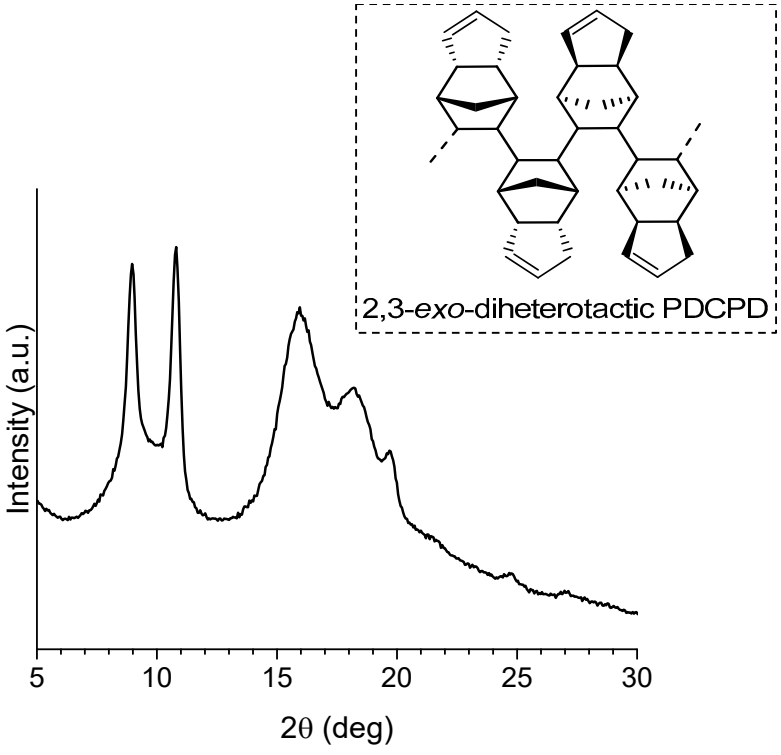

Figure 8. X-ray powder diffraction profile of entry 6.

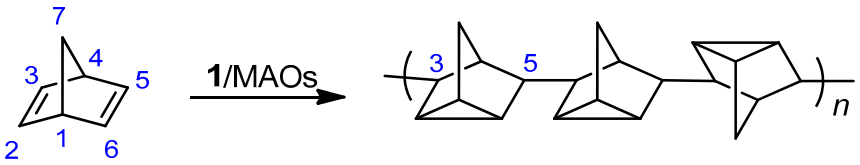

Scheme 4. Polymerization of norbornadiene.

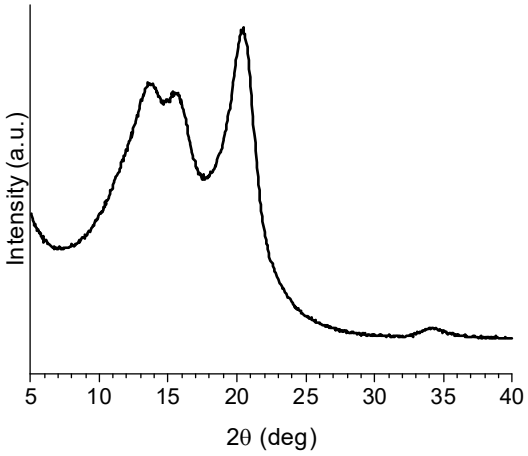

Figure 9. X-ray powder diffraction profile of entry 8.

TGA experiments were performed also for samples corresponding to entry 6 and 8, indicating that these samples present a thermal stability (T_{onset}) ranging from 340 to 370 °C (Figure S9).

The collected results are in net analogy with those reported by some of the authors for the polymerization of NBD mediated by the catalytic system $TiCl_4/Et_2AlCl$ [48]. It is likely that the polymer is obtained through a transannular cationic polymerization of NBD involving both double bonds (Scheme 4), rather than through vinyl-type addition previously observed with NB and its other derivatives. This mechanistic path generally involves the formation of a carbocation on the monomer, which drives the polymerization (Scheme S1). The generation of the carbocationic species may be caused by the cationic Cr-alkyl active species when the Cr complex and MAOs are mixed.

2.4. Characterization of the Activated Complexes

The catalytic tests described above with Al-activated complexes **1** and **2** are not influenced by the coordination mode of Cr(III) to the ligand. To better understand the reasons why the two complexes behave in the same (or very similar) way, we performed a detailed investigation of the effect of the activator on the vibrational/electronic properties of the two complexes. Seeking to avoid the ambiguities of MAO chemistry, we set out to explore the reactivity of the two complexes with triethyl aluminum (TEAl, Et_3Al).

Figure 10 shows the evolution of the IR spectra of the two complexes in the presence of TEAl. Quite interestingly, upon addition of 10 μL of TEAl, the IR spectrum of complex **1** (spectrum 1a) turns out to be very similar to the spectrum of complex **2**. In particular, the intense band at 1540 cm^{-1} characteristic for the ν(C=O) vibration of the metal chelated carbonyl disappears, while a prominent band arises at 1510 cm^{-1}, the same observed in the spectrum of complex **2** and ascribed to the ν(C=N) vibration of the metal chelated imine. Simultaneously, the band at 1318 cm^{-1}, assigned to the ν(C–N) vibration of the N–Ph group in complex **1** shifts at 1394 cm^{-1}, where the same vibration is observed for complex **2**. The subsequent addition of a second dose of TEAl (30 μL) causes further changes in the IR spectrum of complex **1** (spectrum 1b): the band at 1510 cm^{-1} is abated, while a new band appears around 1635 cm^{-1}, the latter attributed to the ν(C=N) vibration of non-interacting imine group [49]. That transformation, also observed upon interacting complex **2** with

10 μL of TEAl (spectrum 2a), can be thus associated with a detachment of the imine nitrogen from Cr.

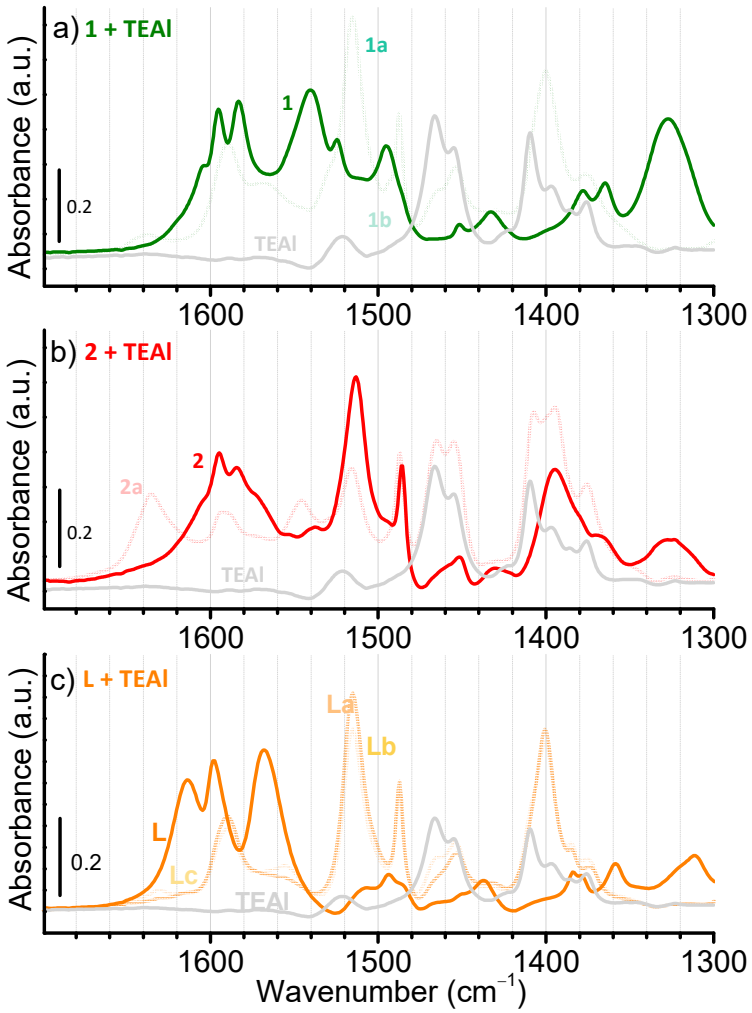

Figure 10. Evolution of transmission IR spectra of complex **1** (**a**, green lines), complex **2** (**b**, red lines), and ligand **L** (**c**) in the presence of increasing amounts of TEAl (10 μL for 1a, 2a and La; 20 μL for Lb, and 30 μL for 1b and Lc). The spectra have been collected in chloroform solution at a concentration of 5×10^{-3} M, and the contribution of the solvent was subtracted from all the spectra. Also, the spectrum of neat TEAl is reported for comparison (grey line).

Hence, from a spectroscopic point of view, after the interaction of the complexes with TEAl, we obtained two IR spectra (1b and 2a) that are superimposable, showing that the catalytically active species are analogous to each other. We postulated that, for this to happen, the ligand should be deprotonated and then covalently bonded to the metal. To confirm this hypothesis, a blank experiment was conducted where increasing amounts of TEAl (10, 20, and 30 μL) were progressively added to the ligand in chloroform solution (5×10^{-3} M). The results are reported in Figure 10c. The IR spectrum of **L** in chloroform solution is very similar to that of **L** in solid state, already discussed in Figure 2. After the addition of 10 μL of TEAl, the spectrum drastically changes. The absorption bands in the 1640–1540 cm^{-1} region are abated, while new sharp bands appear at 1510 and 1487 cm^{-1}, which are characteristic for ν(C=N) of deprotonated **L**$^{-}$ after metallation. Since the only metal present in this case is Al, it is likely that **L**$^{-}$ is stabilized by formation of a covalent Al-O bond, giving rise to a complex resembling complex **2**. Upon further addition of TEAl (20 and 30 μL) these bands decrease in intensity in favor of a weak band at 1635 cm^{-1}, which can be assigned to the same ν(C=N) vibration, but for an imine group no longer interacting

with the metal [49]. This is very similar to what was observed upon adding 10 µL of TEAl to complex **2** and 30 µL of TEAl to complex **1** and can be explained by considering the "displacement" of the nitrogen of the imine group from the metal (either Cr or Al, depending on the case), induced by the presence of sterically encumbering TEAl-dimers (or their derivatives) in the coordination sphere of the metal. This was further demonstrated by some data previously reported in the literature: indeed, the reaction between an Al-alkyl compound and a ketoimine ligand was performed to successfully synthesize aluminum ketiminate complexes, [25] thus proving that AlR_3 is able to deprotonate the ligand.

Complementary UV-Vis experiments (reported in Figure S10) are consistent with the results obtained by IR spectroscopy.

3. Materials and Methods

3.1. General Procedures and Material

Manipulations of air- and/or moisture-sensitive materials were carried out under an inert atmosphere using a dual vacuum/nitrogen line and standard Schlenk-line techniques with oven-dried glassware. Nitrogen and ethylene were purified by passage over columns of $CaCl_2$, molecular sieves, and BTS catalysts. THF (Aldrich, Merck KGaA (Darmstadt, Germany), ≥99.9%) was refluxed over Na/benzophenone alloy for 8 h and then distilled and stored over molecular sieves. Toluene (Aldrich, Merck KGaA (Darmstadt, Germany), >99.5%) was refluxed over Na for 8 h and then distilled and stored over molecular sieves. Pentane (Aldrich, Merck KGaA (Darmstadt, Germany), >99%) was refluxed over Na/K alloy for 8 h and then distilled and stored over molecular sieves. Dichloromethane (Aldrich, Merck KGaA (Darmstadt, Germany), ≥99.9%) was dried by stirring over CaH_2 in an inert atmosphere for 8 h, distilled, and stored over 5 Å molecular sieves away from bright light. NB (Aldrich, Merck KGaA (Darmstadt, Germany), 99% pure) was stirred over molten potassium at 80 °C under nitrogen for 4 h and then distilled. A stock solution was prepared by dissolving 50 g of freshly distilled NB in 86.2 mL of toluene. DCPD (Aldrich, Merck KGaA (Darmstadt, Germany), 95%), ENB (mixture of endo and exo, Aldrich, Merck KGaA (Darmstadt, Germany), 99%), NBD (Aldrich, Merck KGaA (Darmstadt, Germany), 98%) were dried over CaH_2 at 60 °C under nitrogen for 4 h and then distilled under reduced pressure. MAO (Aldrich, Merck KGaA (Darmstadt, Germany), 7 wt% solution in toluene), diethylaluminum chloride (Et_2AlCl, Aldrich, Merck KGaA (Darmstadt, Germany), 97%), $CrCl_2$ (Aldrich, Merck KGaA (Darmstadt, Germany) 99.99%), *n*-buthillithium (*n*BuLi, 1.6 M in hexane, Aldrich, Merck KGaA (Darmstadt, Germany)), and deuterated solvent for NMR measurements ($C_2D_2Cl_4$) (Aldrich, Merck KGaA (Darmstadt, Germany), >99.5% atom D) were used as received. $CrCl_3(THF)_3$ was prepared through the Soxhlet extraction of anhydrous $CrCl_3$ with boiling THF and the aid of Zn dust.

3.2. Synthesis of the Ligand

4-(Phenylimino)-pentan-2-one was synthesized by a procedure similar to the general procedure for the preparation of imines from carbonyl compounds [33]. Acetyl acetone (1.0 mL, 1.0 g, 0.01 mol) was dissolved in toluene (6 mL); then aniline (1.1 mL, 1.1 g, 0.012 mol) and a few drops of acetic acid were added. The flask was equipped with 5 Å molecular sieves to remove water. The reaction mixture was refluxed for 4 h. Then the reaction mixture was cooled, and the solvent distilled off in vacuum. The resulting yellow oil was purified by recrystallization from a cold hexane-methylene chloride mixture (30 mL) (5% by volume). Yield: 0.98 g (56%). The ligand was characterized by ^{1}H NMR spectroscopy: δ 3.17 (s, 3H), 3,25 (s, 3H), 6.36 (s, 1H), 8.25-8.55 (m, 5H), 13.63 (broad, 1H); the NMR spectrum shows that the ligand in its enolic form (Figure S1).

3.3. Synthesis of the Cr complexes

3.3.1. Synthesis of Chromium Complex **1**

In a 250 mL round-bottomed flask equipped with a magnetic stirrer, $CrCl_3(THF)_3$ (2.4 mmol, 0.9 g) was suspended in 60 mL of dry THF at room temperature, and the ligand

(5.5 mmol, 0.96 g) was added as THF solution (10 mL). The suspension was stirred for 24 h, and then the solvent was partially removed in vacuum and filtered off. The residue on the filter was thoroughly washed with dry pentane (3 × 50 mL), dried under vacuum, and stored under nitrogen in a Schlenk tube. After drying, a light green solid was isolated. Yield (based on $CrCl_3(THF)_3$): 78%. Anal. Calcd for $C_{22}H_{26}Cl_3CrN_2O_2$: C, 51,23; H, 5.15; N, 5.51. Found: C, 53.68; H, 5.62; N, 5.42.

3.3.2. Synthesis of Chromium Complex **2**

The synthesis was performed according to the synthetic procedure reported for analogous compounds [50]. $CrCl_3(THF)_3$ (2.08 mmol, 0.78 g) was suspended in dry THF (50 mL). A solution of *n*BuLi (1.6 M in hexane, 2 mL, 3.12 mmol) was added dropwise to a stirred solution of the ligand (3.12 mmol, 0.5 g) in dry THF (10 mL) at 0 °C. The mixture was slowly warmed to room temperature and stirred for 1 h, then was channeled to the solution of $CrCl_3(THF)_3$. The mixture was continuously stirred overnight at room temperature. A green solution was obtained, and the solvent was removed under vacuum. The greenish solid was suspended in dry pentane, filtered and washed with dry pentane (3 × 50 mL), dried under vacuum, and stored under nitrogen in a Schlenk tube. Yield (based on $CrCl_3(THF)_3$): 92%. Anal. Calcd for $C_{11}H_{13}Cl_2CrNO$: C, 44.32; H, 4.40; N, 4.70. Found: C, 43.71; H, 4.88; N, 3.97.

3.4. Polymerization Procedure

Polymerization of ethylene was carried out in a 50 mL round-bottomed Schlenk flask, while the polymerization of cyclic olefins (NB, DCPD, ENB, and NBD) was carried out in a 25 mL Schlenk tube. Before starting the polymerization, the reactor was heated to 110 °C under vacuum for 1 h and back-filled with nitrogen. For the polymerization of ethylene, the reactor was charged at room temperature with toluene and the cocatalyst in that order. After thermal equilibration at the desired temperature, the solution was degassed, and ethylene was added until saturation. Polymerization was started by adding a toluene solution (2 mg mL^{-1}) of the chromium complex via syringe under a continuous flow of ethylene (1.01 bar). For the polymerization of cyclic olefins, the monomer and toluene were transferred into the reactor, the solution was brought to the desired polymerization temperature, and then the cocatalyst and a toluene solution (2 mg mL^{-1}) of the chromium complex were added in that order. Polymerizations were stopped with methanol containing a small amount of hydrochloric acid; the precipitated polymers were collected by filtration, repeatedly washed with fresh methanol, and finally dried under vacuum at room temperature to constant weight.

In all of the reactions investigated, no polymerization activity was observed in the absence of a chromium source.

3.5. Characterization Methods

Elemental analyses were performed using a Perkin–Elmer (Waltham, MA, USA) CHN Analyzer 2400 Series II at the Laboratoire de Chimie de Coordination (Toulouse, France) (C,H,N). FT-IR and UV−Vis−NIR spectra of precatalysts **1** and **2** were measured in transmission mode by dissolving the complexes in chloroform (10^{-3} and 10^{-4} mol L^{-1}) and after adding increasing amounts of TEAl (10, 20, and 30 µL). FT-IR spectra were collected in the spectral range of 7000−400 cm^{-1}, using a Bruker (Bruker AXS Inc., Madison, WI, USA) Alpha spectrophotometer that was placed inside the glovebox to avoid sample contamination. The solutions were measured in a Specac Omni cell equipped with KBr windows. UV-Vis-NIR spectra were collected using a Cary5000 spectrophotometer; the solutions were measured inside homemade cells equipped with windows in optical quartz (Suprasil), filled inside the glovebox, and closed with Teflon plugs. For both techniques, the spectrum of the solvent was recorded under the same conditions and subtracted from those of the samples. FT-IR spectra of the organometallic compounds in powder form were acquired in attenuated total reflectance (ATR) mode, in the spectral range of 7000−400 cm^{-1}, using a

Bruker (Bruker AXS Inc., Madison, WI, USA) Alpha spectrophotometer equipped with a diamond ATR crystal. The measurements were made inside the glovebox to avoid sample contamination.

Far-IR spectra were collected with a Bruker (Bruker AXS Inc., Madison, WI, USA) Vertex70 FT-IR spectrophotometer equipped with a DTGS detector for the Far-IR region. The samples were prepared directly inside a N_2-filled glove-box as thin layers deposited on a highly pure Si wafer (from a suspension in hexane), and placed inside a quartz cell with PE windows, allowing to measure the spectra without exposing the samples to air, as described in Ref. [51]. Far-IR spectra were acquired at a resolution of 4 cm^{-1}, and they are shown after subtracting the weak contributions of both the Si wafer and the PE windows.

ATR–FTIR spectra of the polymers were recorded at room temperature in the 4000–600 cm^{-1} range with a resolution of 4 cm^{-1} using a Perkin-Elmer (Waltham, MA, USA) Spectrum Two spectrometer. NMR spectra were recorded on a Bruker (Bruker AXS Inc., Madison, WI, USA) NMR Advance 400 spectrometer equipped with a SEX 10 mm probe with automatic matching and tuning, operating at 400 MHz (^{1}H) and 100.58 MHz (^{13}C) in the PFT mode at 103 °C. Experiments were performed by dissolving 70 mg of polymer in $C_2D_2Cl_4$ in a 10 mm tube and referenced to HMDS as internal standard. Molecular weight (M_w) and molecular weight distribution (M_w/M_n) were obtained by a high-temperature Waters (Milford, MA, USA) GPCV2000 size exclusion chromatography (SEC) system using an online refractometer detector. The experimental conditions consisted of three PL Gel Olexis columns, o-dichlorobenzene as the mobile phase, 0.8 mL min^{-1} flow rate, and 145 °C temperature. The calibration of the SEC system was constructed using 18 narrow M_w/M_n PS standards with M_w values ranging from 162 to 5.6 × 10^6 g mol^{-1}. For SEC analysis, about 12 mg of the polymer was dissolved in 5 mL of *o*-dichlorobenzene.

Wide-angle X-ray diffraction (XRD) experiments were performed with a Malvern Panalytical (Malvern, UK) Empyrean multipurpose diffractometer using Cu Kα radiation (λ = 1.5418 Å) by a continuous scan of the diffraction angle 2θ in the interval 5–40° at a speed of 0.05252°/s.

Differential scanning calorimetry (DSC) measurements were performed with a Mettler (Columbus, OH, USA) DSC822 operating in a N_2 atmosphere. The sample, typically 5 mg, was placed in a sealed aluminum pan, and the measurement was performed from −70 to 180 °C using a heating and cooling rate of 10 °C min^{-1}. T_m and ΔH_m values were recorded during the second heating.

Thermogravimetric analysis (TGA) was carried using a Perkin-Elmer (Waltham, MA, USA) TA4000 instrument at a heating rate of 10 °C min^{-1} under a flowing N_2 atmosphere in the temperature range 30–900 °C.

4. Conclusions

Two chromium complexes bearing a β-ketoimine ligand were synthesized from $CrCl_3(THF)_3$ according to two different routes: in complex **1** the ligand is coordinated to the metal in the neutral form, while complex **2** was obtained with the lithium salt of the same ligand. Characterization of the two complexes by elemental analysis, IR and UV-Vis spectroscopies, revealed that complex **1** is surrounded by two ligands, with the two O atoms coordinated to Cr, while in complex **2** only one ligand is present, covalently bonded to Cr through the O atom and with the N atom chelated to the metal by coordination.

When activated with MAO, both the complexes are poorly active in the polymerization of ethylene. By contrast, high productivities were reached in the polymerization of various cyclic olefins, with the only exception of bulky DCPD. Vinyl-enchained, stereoregular, semicrystalline oligomers were obtained, particularly in the case of NB and DCPD, while the polymerization of NBD gave a polymer with unique repeating 3,5-enchained nortricyclene units.

Since the nature of the metal-ligand bond does not influence the results of the polymerization, with the complexes being almost equally active, we investigated at a molecular level their activated form in combination with the Al-cocatalyst (either MAO or TEAl). The

activated complexes showed comparable spectra, indicative of the presence of a covalent bond between the O atom of the ligand and the Cr center and of an imine group non-interacting with the metal. Blank experiments performed on the ligand alone demonstrated that this is because TEAl can deprotonate the ligand, bringing to a final situation that is analogous for both the complexes.

Taken together, our results indicate that **1** and **2** are different in principle, but once activated they exhibit similar spectroscopic features and the same catalytic behavior in the polymerization of ethylene and various cyclic olefins. It is worth noting that the substituents on the β-ketoimines largely affect the acidity of the α-proton on the ligand, thus preventing a generalization of the behavior of β-ketoimines different from that employed in this study.

Supplementary Materials: The following supporting information can be downloaded at: https://www.mdpi.com/article/10.3390/catal12020119/s1. Figure S1: ^{1}H NMR spectrum of ligand **L**; Figure S2: X-ray powder diffraction profiles of PE samples; Figure S3: FTIR of poly(norbornene); Figure S4: FTIR of poly(diciclopentadiene) and poly(5-ethylidene-2-norbornene); Figure S5: ^{1}H and ^{13}C NMR of poly(diciclopentadiene); Figure S6: ^{1}H and ^{13}C NMR of poly(5-ethylidene-2-norbornene); Figure S7: TGA curves of the poly(norbornene); Figure S8: FTIR of poly(norbornadiene); Figure S9: TGA curves of poly(diciclopentadiene) and poly(norbornadiene) samples; Figure S10: evolution of the UV-Vis spectra of complexes **1** and **2** in the presence of TEAl. Table S1: data concerning the polymerization of ethylene. Scheme S1: mechanistic pathway of the polymerization of norbornadiene.

Author Contributions: Conceptualization, Synthesis, Data Curation, Writing—original draft preparation and review, G.Z.; Ligand and Complex characterization, Writing—original draft preparation, A.A., A.P. and V.G.; Polymerization experiments, B.P.; Polymer characterization, Writing—original draft preparation, F.D.S.; Supervision, Project Administration and Funding Acquisition, G.L., R.D.G. and E.G. All authors have read and agreed to the published version of the manuscript.

Funding: This work was supported by the project "*Cr4FUN—Chromium catalysis: from fundamental understanding to functional aliphatic polymers*" funded by MIUR Progetti di Ricerca di Rilevante Interesse Nazionale (PRIN) Bando 2017 (20179FKR77_002).

Data Availability Statement: Not applicable.

Acknowledgments: The authors thank Fulvia Greco and Daniele Piovani for skilled technical assistance. G.Z., B.P., A.A., A.P., and F.D.S. thank the project "*Cr4FUN—Chromium catalysis: from fundamental understanding to functional aliphatic polymers*" funded by MIUR Progetti di Ricerca di Rilevante Interesse Nazionale (PRIN) Bando 2017 (20179FKR77_002) for PhD and post-doc grants.

Conflicts of Interest: The authors declare no conflict of interest.

References

1. Holm, R.H.; Chakravorty, A.; Everett, G.W. Metal Complexes of Schiff Bases and β-Ketoamines. *Prog. Inorg. Chem.* **1966**, *7*, 83–214.
2. Mehrotra, R.C.; Bohra, R.; Gaur, D.P. *Metal β-Diketonates and Allied Derivatives*; Academic Press: New York, NY, USA, 1978.
3. Bourget-Merle, L.; Lappert, M.F.; Severn, J.R. The Chemistry of β-Diketiminatometal Complexes. *Chem. Rev.* **2002**, *102*, 3031–3065. [CrossRef]
4. Chamberlain, B.M.; Cheng, M.; Moore, D.R.; Ovitt, T.M.; Lobkovsky, E.B.; Coates, G.W. Polymerization of lactide with zinc and magnesium β-diiminate complexes: Stereocontrol and mechanism. *J. Am. Chem. Soc.* **2001**, *123*, 3229–3238. [CrossRef] [PubMed]
5. Hayes, P.G.; Piers, W.E.; McDonald, R. Cationic scandium methyl complexes supported by a β-diketiminato ("Nacnac") ligand framework. *J. Am. Chem. Soc.* **2002**, *124*, 2132–2133. [CrossRef] [PubMed]
6. Kim, W.K.; Fevola, M.J.; Liable-Sands, L.M.; Rheingold, A.L.; Theopold, K.H. [$(Ph)_2$nacnac]$MCl_2(THF)_2$ (M = Ti, V, Cr): A new class of homogeneous olefin polymerization catalysts featuring β-diiminate ligands. *Organometallics* **1998**, *17*, 4541–4543. [CrossRef]
7. MacAdams, L.A.; Kim, W.K.; Liable-Sands, L.M.; Guzei, I.A.; Rheingold, A.L.; Theopold, K.H. The $(Ph)_2$nacnac ligand in organochromium chemistry. *Organometallics* **2002**, *21*, 952–960. [CrossRef]
8. Holland, P.L.; Tolman, W.B. Three-coordinate Cu(II) complexes: Structural models of trigonal-planar type 1 copper protein active sites. *J. Am. Chem. Soc.* **1999**, *121*, 7270–7271. [CrossRef]
9. Basuli, F.; Bailey, B.C.; Tomaszewski, J.; Huffman, J.C.; Mindiola, D.J. A terminal and four-coordinate titanium alkylidene prepared by oxidatively induced α-hydrogen abstraction. *J. Am. Chem. Soc.* **2003**, *125*, 6052–6053. [CrossRef]
10. Kogut, E.; Wiencko, H.L.; Zhang, L.; Cordeau, D.E.; Warren, T.H. A Terminal Ni(III)-Imide with Diverse Reactivity Pathways. *J. Am. Chem. Soc.* **2005**, *127*, 11248–11249. [CrossRef]

11. MacLeod, K.C.; Vinyard, D.J.; Holland, P.L. A multi-iron system capable of rapid N_2 formation and N_2 cleavage. *J. Am. Chem. Soc.* **2014**, *136*, 10226–10229. [CrossRef]
12. Thompson, R.; Chen, C.-H.; Pink, M.; Wu, G.; Mindiola, D.J. A Nitrido Salt Reagent of Titanium Scheme 1. Synthetic Protocol for the Parent Imido 2 and Nitride 3. *J. Am. Chem. Soc.* **2014**, *136*, 8197–8220. [CrossRef]
13. Jang, E.S.; McMullin, C.L.; Käß, M.; Meyer, K.; Cundari, T.R.; Warren, T.H. Copper(II) anilides in sp^3 C-H amination. *J. Am. Chem. Soc.* **2014**, *136*, 10930–10940. [CrossRef]
14. Radwan, Y.K.; Maity, A.; Teets, T.S. Manipulating the Excited States of Cyclometalated Iridium Complexes with β-Ketoiminate and β-Diketiminate Ligands. *Inorg. Chem.* **2015**, *54*, 7122–7131. [CrossRef] [PubMed]
15. Maya, R.A.; Maity, A.; Teets, T.S. Fluorination of Cyclometalated Iridium β-Ketoiminate and β-Diketiminate Complexes: Extreme Redox Tuning and Ligand-Centered Excited States. *Organometallics* **2016**, *35*, 2890–2899. [CrossRef]
16. Lai, P.N.; Brysacz, C.H.; Alam, M.K.; Ayoub, N.A.; Gray, T.G.; Bao, J.; Teets, T.S. Highly Efficient Red-Emitting Bis-Cyclometalated Iridium Complexes. *J. Am. Chem. Soc.* **2018**, *140*, 10198–10207. [CrossRef] [PubMed]
17. Yersin, H. *(Hartmut) Highly Efficient OLEDs with Phosphorescent Materials*; John Wiley & Sons: Hoboken, NJ, USA, 2007; p. 438.
18. Mehrotra, R.C. Chemistry of metal β-diketonates. *Pure Appl. Chem.* **1988**, *60*, 1349–1356. [CrossRef]
19. Gibson, D. Carbon-bonded beta-diketone complexes. *Coord. Chem. Rev.* **1969**, *4*, 225–240. [CrossRef]
20. Arslan, E.; Lalancette, R.A.; Bernal, I. An historic and scientific study of the properties of metal(III) tris-acetylacetonates. *Struct. Chem.* **2016**, *1*, 201–212. [CrossRef]
21. Latreche, S.; Schaper, F. Chromium(III) bis(diketiminate) complexes. *Organometallics* **2010**, *29*, 2180–2185. [CrossRef]
22. Govil, N.; Jana, B. A review on aluminum, gallium and indium complexes of (Ph_2-nacnac) ligand. *Inorg. Chim. Acta* **2021**, *515*, 120037. [CrossRef]
23. Li, D.; Peng, Y.; Geng, C.; Liu, K.; Kong, D. Well-controlled ring-opening polymerization of cyclic esters initiated by dialkylaluminum β-diketiminates. *Dalton Trans.* **2013**, *42*, 11295–11303. [CrossRef] [PubMed]
24. Li, X.F.; Dai, K.; Ye, W.P.; Pan, L.; Li, Y.S. New Titanium Complexes with Two β-Enaminoketonato Chelate Ligands: Syntheses, Structures, and Olefin Polymerization Activities. *Organometallics* **2004**, *23*, 1223–1230. [CrossRef]
25. Altaf, C.T.; Wang, H.; Keram, M.; Yang, Y.; Ma, H. Aluminum methyl and isopropoxide complexes with ketiminate ligands: Synthesis, structural characterization and ring-opening polymerization of cyclic esters. *Polyhedron* **2014**, *81*, 11–20. [CrossRef]
26. Jana, B.; Uhl, W. New aluminum and gallium complexes of β-diketiminato and β-ketiminato ligands. *Inorg. Chim. Acta* **2017**, *455*, 61–69. [CrossRef]
27. Bera, S.K.; Panda, S.; Baksi, S.D.; Lahiri, G.K. Redox Non-Innocence and Isomer-Specific Oxidative Functionalization of Ruthenium-Coordinated β-Ketoiminate. *Chem. Asian J.* **2019**, *14*, 4236–4245. [CrossRef] [PubMed]
28. Gibson, V.C.; Newton, C.; Redshaw, C.; Solan, G.A.; White, A.J.P.; Williams, D.J. Synthesis, structures and ethylene polymerisation behaviour of low valent β-diketiminato chromium complexes. *Eur. J. Inorg. Chem.* **2001**, *7*, 1895–1903. [CrossRef]
29. Yoon, S.; Teets, T.S. Red to near-infrared phosphorescent Ir(iii) complexes with electron-rich chelating ligands. *Chem. Commun.* **2021**, *57*, 1975–1988. [CrossRef]
30. Leone, G.; Groppo, E.; Zanchin, G.; Martino, G.A.; Piovano, A.; Bertini, F.; Martí-Rujas, J.; Parisini, E.; Ricci, G. Concerted Electron Transfer in Iminopyridine Chromium Complexes: Ligand Effects on the Polymerization of Various (Di)olefins. *Organometallics* **2018**, *37*, 4827–4840. [CrossRef]
31. Zanchin, G.; Piovano, A.; Amodio, A.; De Stefano, F.; Di Girolamo, R.; Groppo, E.; Leone, G. NEt3-Triggered Synthesis of UHMWPE Using Chromium Complexes Bearing Non-Innocent Iminopyridine Ligands. *Macromolecules* **2021**, *54*, 1243–1253. [CrossRef]
32. Bariashir, C.; Huang, C.; Solan, G.A.; Sun, W.H. Recent advances in homogeneous chromium catalyst design for ethylene tri-, tetra-, oligo- and polymerization. *Coord. Chem. Rev.* **2019**, *385*, 208–229. [CrossRef]
33. Cotton, F.A.; Ilsley, W.H.; Kaim, W. Chelate rings in a quadruply bonded dimetal compound: Preparation and structure of diacetatodi (4-phenylimino-2-pentanonato)dimolybdenum. *Inorg. Chim. Acta* **1979**, *37*, 267–272. [CrossRef]
34. Ueno, K.; Martell, A.E. Infrared Study of Metal Chelates of Bisacetylacetone-Ethylidenediimine and Related Compounds. *J. Phys. Chem.* **1955**, *59*, 998–1004. [CrossRef]
35. Camp, C.; Arnold, J. On the non-innocence of "Nacnacs": Ligand-based reactivity in β-diketiminate supported coordination compounds. *Dalton Trans.* **2016**, *45*, 14462–14498. [CrossRef] [PubMed]
36. Fujita, J.; Martell, A.E.; Nakamoto, K. Infrared spectra of metal chelate compounds. VI. A normal coordinate treatment of oxalato metal complexes. *J. Chem. Phys.* **1962**, *36*, 324–331. [CrossRef]
37. Ferraro, J.R. *Low-Frequency Vibrations of Inorganic and Coordination Compounds*; Springer: Boston, MA, USA, 1971.
38. Chatt, J.; Hayter, R.G. Ligand Field Strengths of the Halide, Methyl, Phenyl, and Hydride Anions. *J. Chem. Soc.* **1961**, *167*, 772–774. [CrossRef]
39. Figgis, B.N. *Introduction to Ligand Fields*; John Wiley & Sons, Ltd.: New York, NY, USA, 1966.
40. Bermeshev, M.V.; Chapala, P.P. Addition polymerization of functionalized norbornenes as a powerful tool for assembling molecular moieties of new polymers with versatile properties. *Prog. Polym. Sci.* **2018**, *84*, 1–46. [CrossRef]
41. Zanchin, G.; Leone, G. Polyolefin thermoplastic elastomers from polymerization catalysis: Advantages, pitfalls and future challenges. *Prog. Polym. Sci.* **2021**, *113*, 101342. [CrossRef]

42. Rapallo, A.; Porzio, W.; Zanchin, G.; Ricci, G.; Leone, G. 2,3-exo-Diheterotactic Dicyclopentadiene Oligomers: An X-ray Powder Diffraction Study of a Challenging Multiphase Case. *Chem. Mater.* **2019**, *31*, 6650–6664. [CrossRef]
43. Blank, F.; Janiak, C. Metal catalysts for the vinyl/addition polymerization of norbornene. *Coord. Chem. Rev.* **2009**, *253*, 827–861. [CrossRef]
44. Ricci, G.; Boglia, A.; Boccia, A.C.; Zetta, L.; Famulari, A.; Meille, S.V. New stereoregularity in the stereospecific polymerization of bulky strained olefins: Diheterotactic polynorbornene. *Macromolecules* **2008**, *41*, 3109–3113. [CrossRef]
45. Zanchin, G.; Leone, G.; Pierro, I.; Rapallo, A.; Porzio, W.; Bertini, F.; Ricci, G. Addition Oligomerization of Dicyclopentadiene: Reactivity of Endo and Exo Isomers and Postmodification. *Macromol. Chem. Phys.* **2017**, *218*, 1600602. [CrossRef]
46. Arndt, M.; Engehausen, R.; Kaminsky, W.; Zoumis, K. Hydrooligomerization of cycloolefins -a view of the microstructure of polynorbornene. *J. Mol. Catal. A Chem.* **1995**, *101*, 171–178. [CrossRef]
47. Roller, M.B.; Gillham, J.K.; Kennedy, J.P. Thermomechanical Behavior of a Polynorbornadiene. *J. Appl. Polym. Sci.* **1973**, *17*, 2223–2233. [CrossRef]
48. De Rosa, C.; Malafronte, A.; Auriemma, F.; Scoti, M.; Di Girolamo, R.; D'Alterio, M.C.; Ricci, G.; Zanchin, G.; Leone, G. Synthesis, chain conformation and crystal structure of poly(norbornadiene) having repeating 3,5-enchained nortricyclene units. *Polym. Chem.* **2019**, *10*, 4593–4603. [CrossRef]
49. Fabian, J.; Legrand, M.; Poirier, P. L'etude spectrographique infrarouge et Raman du groupe imine. *Bull. Soc. Chim. Fr.* **1956**, *10*, 1499–1509.
50. Huang, Y.B.; Jin, G.X. Half-sandwich chromium(III) complexes bearing β-ketoiminato and β-diketiminate ligands as catalysts for ethylene polymerization. *Dalton Trans.* **2009**, *5*, 767–769. [CrossRef] [PubMed]
51. Piovano, A.; Zarupski, J.; Groppo, E. Disclosing the Interaction between Carbon Monoxide and Alkylated Ti^{3+} Species: A Direct Insight into Ziegler-Natta Catalysis. *J. Phys. Chem. Lett.* **2020**, *11*, 5632–5637. [CrossRef]